Inorganic Chemistry

Article

pubs.acs.org/IC

Do Solid-State Structures Reflect Lewis Acidity Trends of Heavier Group 13 Trihalides? Experimental and Theoretical Case Study

Alexey Y. Timoshkin,*[,†] Michael Bodensteiner,[‡] Tatiana N. Sevastianova,[†] Anna S. Lisovenko,[†] Elena I. Davydova,[†] Manfred Scheer,[‡] Christian Graßl,[‡] and Alina V. Butlak[†]

[†]Inorganic Chemistry Group, Department of Chemistry, St. Petersburg State University, University Pr. 26, Old Peterhof, St. Petersburg 198504, Russia

[‡]Department of Inorganic Chemistry, University of Regensburg, 93040 Regensburg, Germany

Supporting Information

ABSTRACT: Lewis acidity trends of aluminum and gallium halides have been considered on the basis of joint X-ray and density functional theory studies. Structures of complexes of heavier group 13 element trihalides MX_3 (M = Al, Ga; X = Cl, Br, I) with monodentate nitrogen-containing donors Py, pip, and NEt_3 as well as the structure of the $AlCl_3{\cdot}PPh_3$ adduct have been established for the first time by X-ray diffraction studies. Extensive theoretical studies (B3LYP/TZVP level of theory) of structurally characterized complexes between MX_3 and nitrogen-, phosphorus-, arsenic-, and oxygen-containing donor ligands have allowed us to establish the Lewis acidity trends Al > Ga, Cl ≈ Br > I. Analysis of the experimental and theoretical results points out that the solid state masks the Lewis acidity trend of aluminum halides. The difference in the Al−N bond distances between $AlCl_3{\cdot}D$ and $AlBr_3{\cdot}D$ complexes in the gas phase is small, while in the condensed phase, shorter Al−N distances for $AlBr_3{\cdot}D$ complexes are observed with 9-fluorenone, mdta, and NEt_3 donors. The model based on intermolecular (H···X) interactions in solid adducts is proposed to explain this phenomenon. Thus, the donor−acceptor bond distance in the solid complexes cannot always be used as a criterion of Lewis acidity.

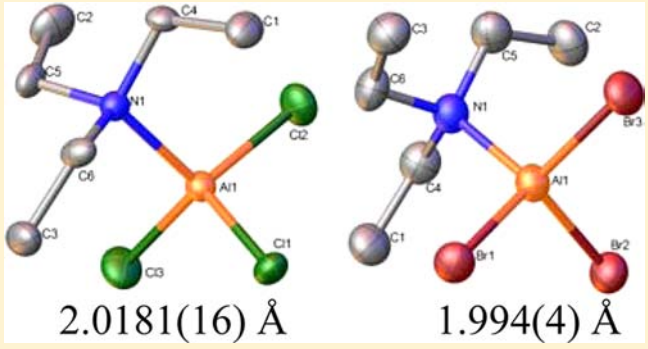

INTRODUCTION

Lewis acid−base interactions are widespread in modern chemistry. Although qualitative definitions of Lewis acids and bases[1] are quite simple, quantification of the Lewis acidity and basicity is a challenging task. Two common scales are widely used for the Lewis basicity: proton affinities (PAs)[2] and Gutmann's donor numbers (DNs).[3] In contrast, there are no universally adopted quantitative scales of Lewis acidity. There are a number of ways to quantify the Lewis acidity: Gutman's acceptor numbers,[4] Gibbs energy for complex formation (derived from the equilibrium constant measurements in solutions),[5] the length of the donor−acceptor (DA) bond,[6,9] the dissociation enthalpy of the complex in solution[5b] or in the gas phase (as an approximation to the energy of the DA bond),[11] IR band shifts,[10a] DA force constants,[10b,c] electron paramagnetic resonance (EPR)[7] and nuclear quadrupole resonance (NQR) measurements,[9] ^{2}H NMR shifts,[8] and kinetic studies of Lewis acid catalyzed reactions.[8,12] It must be noted that different scales sometimes lead to different orders of Lewis acidity.[13] For example, modern ab initio computations[14] and equilibrium constants of aniline complex formation in dioxane[5b] indicate that $AlCl_3$ is a stronger Lewis acid than $GaCl_3$, but the order is reversed according to EPR experiments.[7]

Group 13 element trihalides MX_3 (M = B, Al, Ga; X = F, Cl, Br, I) are widely used Lewis acids. The Lewis acidity of MX_3 is usually compared for the series of complex compounds featuring the same Lewis base. While the increase of the Lewis acidity of boron halides $BF_3 < BCl_3 < BBr_3 < BI_3$ is well established and explained on the basis of recent theoretical works,[15] the influence of the halogen atom on the Lewis acidity of heavier group 13 element halides remains controversial. According to the equilibrium constant for an aniline complex formation in a diethyl ether solution, $AlBr_3$ is a stronger Lewis acid than $AlCl_3$.[5a] A comparative study of the Lewis acidity with respect to 9-fluorenone indicates $AlBr_3$ as the stronger Lewis acid on the basis of the IR shift in the C═O stretching mode, ^{1}H NMR equilibrium constant measurements, and Al−O bond distances.[13] However, at the same time, ^{13}C NMR measurements (downfield shift of C═O carbon) indicate $AlCl_3$ as a stronger Lewis acid than $AlBr_3$.[13] For gallium halides, the Ga−O bond distances, IR shifts, and ^{13}C NMR data suggest that $GaCl_3$ is a stronger Lewis acid than $GaBr_3$,[13] while the opposite trend is found on the basis of dissociation enthalpies and equilibrium

Received: July 13, 2012
Published: October 9, 2012

dx.doi.org/10.1021/ic301507c | Inorg. Chem. 2012, 51, 11602−11611

Table 1. Experimental and Theoretically Predicted DA Bond Distances (R_{M-N}, Å) and Dissociation Enthalpies ($\Delta_{diss}H°$, kJ mol^{-1}) for Gas-Phase Complexes of Group 13 Metal Halides with Ammonia

		R_{M-N}		$\Delta_{diss}H°$	
complex		X = Cl	X = Br	X = Cl	X = Br
$AlX_3{\cdot}NH_3$	exp	1.996 ± 0.019[19]	1.997 ± 0.019[17]	137.2 ± 3.8[20,21]	143.9 ± 4.6[22]
	theor[a]	2.012	2.022	156.7	148.3
$GaX_3{\cdot}NH_3$	exp	2.057 ± 0.011[18]	2.081 ± 0.023[17]	134.3 ± 0.8[21,23]	137.2 ± 0.8[23]
	theor[a]	2.065	2.072	134.2	123.8

[a]B3LYP/LANL2DZ(d,p) level of theory.[16]

Table 2. Experimental DA Bond Distances for $X_3M{\cdot}D$ Adducts in the Solid State (Å) and PAs of the Respective Donor Molecules (kJ mol^{-1})

DA bond	complex	X = Cl	X = Br	X = I	PA[44]
Al−N	$AlX_3{\cdot}NH_3$	1.921(3)[26]	1.918(17),[26] 1.925(17)[26]	1.957(19)[26]	853.6
	$AlX_3{\cdot}Py$	1.930(2)[27]	1.935(3)[a]		930
	$AlX_3{\cdot}tmpH$	2.014(2)[28]	2.009(15)[28]	2.038(9)[28]	987.0
	$AlX_3{\cdot}mdta$	1.993(5)[29]	1.982(5)[29]		898[b]
	$AlX_3{\cdot}NEt_3$	2.0181(16)[a]	1.994(4),[a] 1.973(8)[30]		981.8
Al−P	$AlX_3{\cdot}P(SiMe_3)_3$	2.392(4)[31]	2.391(6)[31]		996[b]
	$AlX_3{\cdot}PPh_3$	2.4296(15)[a]			972.8
Al−O	$AlX_3{\cdot}O{=}PPh_3$	1.733(4)[32]	1.736(7)[32]		906.2
	$AlX_3{\cdot}THF$	1.798(6)[33]	1.823(8)[34]		822.1
	$AlX_3{\cdot}9$-fluorenone	1.787(3)[35]	1.756(9)[13]		874[b]
Al−C	$AlX_3{\cdot}IMes$		2.0168(17)[42a]	2.035(3)[42b]	
Ga−C	$GaX_3{\cdot}IMes$	1.954(4)[42c]	2.006(8)[42d]		
Ga−O	$GaX_3{\cdot}9$-fluorenone	1.915(2)[13]	1.936(4)[13]		874[b]
Ga−N	$GaX_3{\cdot}Py$	1.9660(1)[a]	1.979(2)[a]	2.000(4)[a]	930
	$GaX_3{\cdot}pip$	1.975(1)[a]			954
Ga−P	$GaX_3{\cdot}PPh_3$	2.3717(16)[36]	2.3848(13),[36] 2.3879(13)	2.413(4),[37] 2.416(6)[38]	972.8
	$GaX_3{\cdot}P(SiMe_3)_3$	2.379(5),[39] 2.380(5)[39]	2.362(4)[39]	2.347(4)[39]	996[b]
	$GaX_3{\cdot}dppe{\cdot}GaX_3$	2.3854(8)[40]	2.4002(8)[41]	2.404(9),[38] 2.410(9)	
Ga−As	$GaX_3{\cdot}AsMe_3$	2.4332(12)[43]	2.438(2)[43]	2.4593(13)[43]	897.3

[a]Present work. [b]Computed in the present work at the B3LYP/TZVP level of theory.

constants derived from the temperature-dependent ^{1}H NMR measurements.

Comparative computational studies of $MX_3{\cdot}NH_3$ complexes[16] predict that the Lewis acidity of heavier group 13 element halides in the gas phase (derived from both structural and energetic criteria) decreases in the order $MCl_3 > MBr_3 > MI_3$, irrespective of the group 13 metal (M = Al, Ga, In). These theoretical predictions are in agreement with the minor increase of the M−N bond distances in gaseous complexes on going from $MCl_3{\cdot}NH_3$ to $MBr_3{\cdot}NH_3$ found by gas-phase electron diffraction studies.[17−19] While the Al−N DA bond length increases only by 0.001 Å, the difference for the Ga−N bond length is more pronounced: 0.024 Å. Although both differences are small and well within experimental errors (Table 1), they match the theoretically predicted small differences in the Al−N and Ga−N bond lengths between $MBr_3{\cdot}NH_3$ and $MCl_3{\cdot}NH_3$ (0.01 and 0.007 Å, respectively).

In contrast, experimentally derived gas-phase dissociation enthalpies of $MX_3{\cdot}NH_3$ complexes indicate that group 13 metal bromides are slightly stronger Lewis acids than group 13 metal chlorides. The gas-phase dissociation enthalpy $\Delta_{diss}H°$ increases on going from $MCl_3{\cdot}NH_3$ to $MBr_3{\cdot}NH_3$ for both M = Al and Ga (Table 1); indium halides follow the same trend ($\Delta_{diss}H°$ is 112.1 ± 5.4 and 114.2 ± 6.3 kJ mol^{-1} for $InCl_3{\cdot}NH_3$ and $InBr_3{\cdot}NH_3$, respectively[24]).

The length of the DA bond is one of the important characteristics of DA interaction and is one of the criteria of the Lewis acidity used. It is shown that for the large number of molecular complexes there is an inverse relationship between the DA bond energy and Δr. $\Delta r = r_{DA} - a(r_D - r_A)$, where r_{DA} is the DA bond distance and r_D and r_A are covalent radii of the atoms in donor and acceptor molecules.[25] Shorter DA bonds usually have larger dissociation energies.[25] In the last 15 years, experimental information on the structures of molecular complexes of group 13 metal halides in the solid state became available and was summarized in a recent review.[21] Analysis of the available experimental structural data for the solid adducts[13,26−42] (Table 2) reveals controversial trends in the Lewis acidity with respect to the halogen.

A very peculiar situation is observed for the aluminum halides. According to the D−A bond distances for the adducts in the solid state (Table 2), $AlBr_3$ is a stronger Lewis acid than $AlCl_3$ toward 9-fluorenone[13] and 5-Me-1,3,5-dithiazinane (mdta).[29] However, the trend is reversed, and $AlCl_3$ is a stronger Lewis acid toward tetrahydrofuran (THF),[33,34] while for complexes of aluminum chloride and bromide with NH_3,[26] tetramethylpiperidine (tmpH),[28] $P(SiMe_3)_3$,[31] and $O{=}PPh_3$,[32] the differences in the D−A bond distances are indistinguishable within experimental errors, indicating the equal Lewis acidity of $AlCl_3$ and $AlBr_3$.

The order of the Lewis acidity of $GaCl_3 > GaBr_3 > GaI_3$ is observed for complexes with PPh_3,[36,37] dppe,[38,40,41] and $AsMe_3$,[43] while the opposite order of $GaCl_3 < GaBr_3 < GaI_3$ is found for complexes with $P(SiMe_3)_3$.[39] There are no solid-state

dx.doi.org/10.1021/ic301507c | Inorg. Chem. 2012, 51, 11602−11611

Table 3. Crystal Structure Information for Investigated Complexes

	$GaCl_3$·Py (**1**)	$GaBr_3$·Py (**2**)	GaI_3·Py (**3**)
empirical formula	$C_5H_5Cl_3GaN$	$C_5H_5Br_3GaN$	$C_5H_5GaI_3N$
M_r	255.17	388.52	529.52
cryst syst	monoclinic	monoclinic	triclinic
space group	$P2_1/n$	$P2_1/n$	$P\bar{1}$
a [Å]	6.3425(2)	6.6618(2)	7.1845(3)
b [Å]	15.9402(5)	16.1465(4)	8.8973(7)
c [Å]	9.1176(3)	9.4029(3)	9.8475(5)
α [deg]	90	90	75.395(6)
β [deg]	103.213(3)	102.686(3)	79.454(4)
γ [deg]	90	90	68.405(6)
V [Å^3]	897.39(5)	986.73(5)	563.53(6)
Z	4	4	2
T [K]	123(1)	123(1)	123(1)
cryst dimens [mm]	0.15 × 0.06 × 0.04	0.19 × 0.03 × 0.03	0.32 × 0.18 × 0.05
ρ_{calcd} [g cm^{-3}]	1.889	2.615	3.121
$F(000)$	496	712	464
abs coeff μ [mm^{-1}]	11.828	17.519	10.601
transmn T_{min}/T_{max}	0.636/1.000	0.194/0.612	0.267/1.000
abs corrn type	multiscan	multiscan	multiscan
device type	Gemini R Ultra CCD	Gemini R Ultra CCD	Gemini R Ultra CCD
wavelength λ [Å]	1.54178 (Cu)	1.54178 (Cu)	0.71073 (Mo)
reflns collected/unique	3327/1559	5481/1721	7082/3113
R_{int} equivalents	0.0306	0.0250	0.0378
unique reflns $I > 2\sigma(I)$	1428	1623	2634
index ranges	$-7 \le h \le 6$	$-6 \le h \le 7$	$-9 \le h \le 9$
	$-18 \le k \le 17$	$-18 \le k \le 19$	$-11 \le k \le 12$
	$-5 \le l \le 10$	$-11 \le l \le 11$	$-13 \le l \le 14$
θ_{min}–θ_{full} [deg]	5.55–66.56	5.48–66.60	2.96–27.50
completeness to θ_{full}	0.982	0.990	0.991
data/restraints/param	1559/0/91	1721/0/111	3113/0/91
final R values (all data)	0.0299/0.0725	0.0247/0.0607	0.0406/0.0714
final R values [$I > 2\sigma(I)$]	0.0270/0.0702	0.0227/0.0596	0.0316/0.0658
GOF on F^2	1.051	1.090	1.043
largest diff $\Delta\rho$ [e Å^{-3}]	−0.362/0.511	−0.614/0.586	−1.306/1.029
Flack parameter			

	GaI_3·Py (**4**)	$GaCl_3$·pip (**5**)	$AlCl_3$·NEt_3 (**6**)
empirical formula	$C_{20}H_{20}Ga_4I_{12}N_4$	$C_5H_{11}Cl_3GaN$	$C_6H_{15}AlCl_3N$
M_r	2118.08	261.22	234.52
cryst syst	monoclinic	triclinic	orthorhombic
space group	$P2_1/c$	$P\bar{1}$	$Pna2_1$
a [Å]	23.8452(6)	6.6198(3)	13.4888(2)
b [Å]	8.5232(2)	8.4213(4)	7.3348(1)
c [Å]	22.3451(5)	9.3591(4)	12.1051(2)
α [deg]	90	85.322(4)	90
β [deg]	90.067(2)	81.826(4)	90
γ [deg]	90	79.284(4)	90
V [Å^3]	4541.36(19)	506.62(4)	1197.65(3)
Z	4	2	4
T [K]	123(1)	123(1)	123(1)
cryst dimens [mm]	0.27 × 0.24 × 0.16	0.62 × 0.38 × 0.30	0.19 × 0.15 × 0.11
ρ_{calcd} [g cm^{-3}]	3.098	1.712	1.301
$F(000)$	3712	260	488
abs coeff μ [mm^{-1}]	10.524	3.442	7.235
transmn T_{min}/T_{max}	0.151/0.320	0.133/0.356	0.385/0.527
abs corrn type	analytical	multiscan	analytical
wavelength λ [Å]	0.71073 (Mo)	0.71073 (Mo)	1.54178 (Cu)
reflns collected/unique	54637/13831	6749/3098	5715/1819
R_{int} equivalents	0.0378	0.0217	0.0247
unique reflns $I > 2\sigma(I)$	10889	2721	1811
index ranges	$-34 \le h \le 33$	$-9 \le h \le 9$	$-15 \le h \le 13$
	$-12 \le k \le 12$	$-12 \le k \le 12$	$-8 \le k \le 7$
	$-30 \le l \le 31$	$-13 \le l \le 13$	$-14 \le l \le 12$
θ_{min}–θ_{full} [deg]	2.56–30.51	3.16–30.51	6.56–64.82
completeness to θ_{full}	0.999	0.999	0.973
data/restraints/param	13831/0/339	3098/0/135	1819/1/113
final R values (all data)	0.0829/0.1761	0.0290/0.0602	0.0222/0.0583
final R values [$I > 2\sigma(I)$]	0.0680/0.1660	0.0243/0.0592	0.0221/0.0580
GOF on F^2	1.035	1.018	1.080
largest diff $\Delta\rho$ [e Å^{-3}]	−8.550/3.707	−0.558/0.559	−0.214/0.162
Flack parameter			−0.009(15)

	$AlBr_3$·NEt_3 (**7**)	$AlCl_3$·PPh_3 (**8**)	$AlBr_3$·Py (**9**)
empirical formula	$C_6H_{15}AlBr_3N$	$C_{18}H_{15}AlCl_3P$	$C_5H_5AlBr_3N$
M_r	367.87	395.60	345.78
cryst syst	orthorhombic	triclinic	monoclinic
space group	$Pna2_1$	$P\bar{1}$	$P2_1/n$
a [Å]	13.4888(2)	9.448(5)	6.6643(1)
b [Å]	7.3348(1)	10.079(5)	16.1144(3)
c [Å]	12.1051(2)	10.315(5)	9.3934(2)
α [deg]	90	105.490(5)	90
β [deg]	90	92.127(5)	102.537(2)
γ [deg]	90	95.719(5)	90
V [Å^3]	1197.65(3)	939.8(8)	984.72(3)
Z	4	2	4
T [K]	123(1)	123(1)	123(1)
cryst dimens [mm]	0.31 × 0.25 × 0.18	0.45 × 0.30 × 0.21	0.18 × 0.15 × 0.03
ρ_{calcd} [g cm^{-3}]	2.040	1.398	2.332
$F(000)$	704	404	640
abs coeff μ [mm^{-1}]	12.806	0.615	15.536
transmn T_{min}/T_{max}	0.031/0.122	0.544/1.000	0.250/0.699
abs corrn type	analytical	multiscan	analytical
wavelength λ [Å]	1.54178 (Cu)	0.71073 (Mo)	1.54178 (Cu)
reflns collected/unique	6048/1518	16717/9278	5559/1709
R_{int} equivalents	0.0308	0.0369	0.0408
unique reflns $I > 2\sigma(I)$	1503	3075	1523
index ranges	$-15 \le h \le 15$	$-11 \le h \le 11$	$-7 \le h \le 7$
	$-8 \le k \le 7$	$-11 \le k \le 11$	$-18 \le k \le 17$
	$-10 \le l \le 13$	$-12 \le l \le 12$	$-11 \le l \le 8$
θ_{min}–θ_{full} [deg]	6.87–60.72	2.05–25.01	5.49–66.60
completeness to θ_{full}	0.982	0.987	0.987
data/restraints/param	1518/1/114	3278/0/208	1709/0/91

dx.doi.org/10.1021/ic301507c | Inorg. Chem. 2012, 51, 11602–11611

Table 3. continued

	$AlBr_3$·NEt_3 (7)	$AlCl_3$·PPh_3 (8)	$AlBr_3$·Py (9)
final R values (all data)	0.0276/0.0637	0.0338/0.0858	0.0273/0.0549
final R values [$I > 2\sigma(I)$]	0.0272/0.0635	0.0317/0.0839	0.0233/0.0527
GOF on F^2	1.119	1.048	1.032
largest diff $\Delta\rho$ [e Å^{-3}]	−0.415/0.354	−0.319/0.347	−0.558/0.410
Flack parameter	0.54(5)		

data for complexes of $GaCl_3$, $GaBr_3$, and GaI_3 with nitrogen-containing donors. Theoretical studies predict a lengthening of the DA bond in GaX_3·Py adducts from chlorides to iodides.[45] Group 13 Lewis acids easily form complexes with pyridine.[54] In earlier studies,[55b] MX_3·nPy complexes (M = Al, Ga; X = Cl, Br, I; n = 1−3) were assumed to be ionic. Experimental X-ray studies of complexes with n = 2 (1:2 composition, MX_3·2Py (M = Al, Ga; X = Cl, Br) showed that they indeed adopt ionic structures $[MX_2Py_4]^+[MX_4]$ in the solid state.[56] However, the complex of 1:1 composition $AlCl_3$·Py has a molecular structure in the solid state.[27] Structural information on complexes of gallium trihalides with pyridine of 1:1 composition is not available.

In an attempt to clarify the order of the Lewis acidity trends for group 13 metal halides, the molecular structures of several complexes of aluminum and gallium halides with monodentate ligands have been determined for the first time by X-ray structural analysis. Temperature-dependent experiments have been carried out for $AlBr_3$·NEt_3. We have also performed extensive theoretical studies on molecular complexes of aluminum and gallium halides with nitrogen-, oxygen-, phosphorus, and arsenic-containing donor ligands, the solid-state structures of which are experimentally known at the present time (Table 2). This joint experimental/theoretical approach allowed us to clarify the Lewis acidity trends of group 13 metal halides.

EXPERIMENTAL DETAILS

Synthesis of Adducts. All complexes have been synthesized by the interaction of equimolar amounts of group 13 element halides with donor molecules in wholeglass apparatus under vacuum. Single crystals suitable for X-ray analysis have been grown by slow sublimation of the complexes in a vacuum.

X-ray Analyses of the Complexes. Crystal structure analyses were performed on an Oxford Diffraction Gemini R Ultra CCD. Either semi-empirical[46] or analytical absorption corrections from crystal faces[47] were applied. The structures were solved by direct and charge-flipping methods using the programs *SIR-97*[48] and *Superflip*,[49] respectively. Full-matrix least-squares refinements on F^2 in *SHELXL-97* were carried out.[50] The hydrogen coordinates were partially refined. **4** turned out to be *pseudo*merohedrally twinned. It is further a polymorph of **3**. In all cases, the largest residual density is located close to the heavy atoms at meaningless positions. CCDC 884018−884026 and 884050−884054 contain the supplementary crystallographic data for this paper. These data can be obtained free of charge from the Cambridge Crystallographic Data Center via http://www.ccdc.cam.ac.uk/products/csd/request/.

Quantum-Chemical Computations. All computations were performed using density functional theory hybrid functional B3LYP[51] in conjunction with a triple-ζ quality basis set with polarization functions. Ahlrichs' all-electron TZVP basis set[52a] was used for boron, aluminum, gallium, carbon, silicon, nitrogen, oxygen, phosphorus, arsenic, fluorine, chlorine, and bromine, the standard 6-311G** basis set[52b] was used for hydrogen, and the effective core potential def2-TZVP basis set[52c] was used for iodine. The B3LYP method has been successfully applied for the complexes of group 13 metal halides with ammonia[16] and provided good agreement with experimental values for dissociation enthalpies. The structures of all compounds were fully optimized and verified to be minima on their respective potential energy surfaces. The *GAUSSIAN 03* program package[53] was used throughout.

RESULTS AND DISCUSSION

Structural Studies. We have been able to grow single crystals of $GaCl_3$·Py (**1**), $GaBr_3$·Py (**2**), GaI_3·Py complexes, the latter of which forms two polymorphs (**3** and **4**), $GaCl_3$·pip (**5**), $AlCl_3$·NEt_3 (**6**), $AlBr_3$·NEt_3 (**7**), $AlCl_3$·PPh_3 (**8**), and $AlBr_3$·Py (**9**) complexes. Experimental details for all complexes are presented in Table 3. All complexes adopt molecular structures in the solid state with a tetrahedral environment at the group 13 element. Their molecular structures and selected structural parameters are presented in Figures 1−8. To get more insight

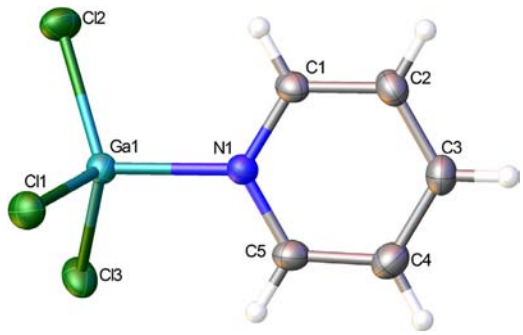

Figure 1. Molecular structure of complex **1** in the crystal. Selected interatomic distances (Å): Ga1−N1 1.966(2), Ga1−Cl1 2.1587(7), Ga1−Cl2 2.1503(7), Ga1−Cl3 2.1598(7). Selected bond angles (deg): Cl1−Ga−Cl2 111.72(3), Cl1−Ga−Cl3 110.09(3), Cl2−Ga−Cl3 112.94(3), Cl1−Ga−N1 107.97(6), Cl2−Ga−N1 108.68(6), Cl3−Ga−N1 105.10(6).

into the issue, extensive quantum-chemical computations of structurally characterized adducts have been carried out, and the results are presented in Table 4. We will start our discussion with trends in the Lewis acidity of gallium halides.

Lewis Acidity Trends of Gallium Trihalides. Our X-ray structure determinations reveal that 1:1 complexes GaX_3·Py [X = Cl (**1**), Br (**2**), I (**3**)] adopt molecular structures in the solid state (Figures 1−3). Two different polymorphs, **3** and **4**, are found for the iodine derivative (Figure S1, Supporting Information). Both are not isostructural to **1** and **2**. Two independent experiments on different single crystals of **3** (GaI_3·Py) yielded similar results.

The Ga−N bond distances in GaX_3·Py complexes determined in the present work increase in the order Cl < Br < I, indicating a $GaCl_3$ > $GaBr_3$ > GaI_3 Lewis acidity trend. The same trend is obtained on the basis of theoretical studies (on both structural and energetic criteria; Table 4). Prior to the present work, the complete set of structural data for gallium trihalides was available only for phosphorus- and arsenic-containing donors. With the single exception of GaX_3·$P(SiMe_3)_3$ complexes, where the "stronger Lewis acidity of the heavier

dx.doi.org/10.1021/ic301507c | *Inorg. Chem.* 2012, 51, 11602−11611

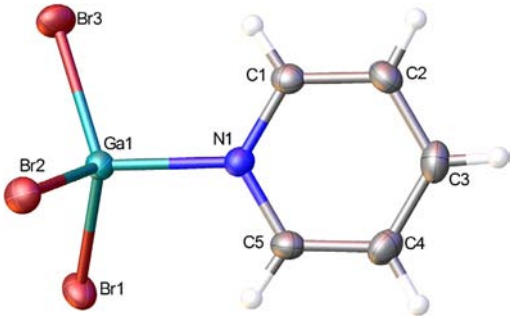

Figure 2. Molecular structure of complex **2** in the crystal. Selected interatomic distances (Å): Ga1−N1 1.979(2), Ga1−Br1 2.3060(5), Ga1−Br2 2.3037(5), Ga1−Br3 2.2948(5). Selected bond angles (deg): Br1−Ga−Br2 110.54(2), Br1−Ga−Br3 113.06(2), Br2−Ga−Br3 112.06(2), Br1−Ga−N1 105.09(8), Br2−Ga−N1 107.40(8), Br3−Ga−N1 108.26(8).

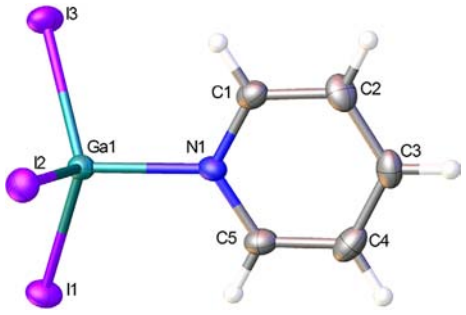

Figure 3. Molecular structure of complex **3** in the crystal. Selected interatomic distances (Å): Ga1−N1 2.000(4), Ga1−I1 2.5246(6), Ga1−I2 2.5106(6), Ga1−I3 2.5191(7). Selected bond angles (deg): I1−Ga−I2 114.07(2), I1−Ga−I3 112.18(2), I2−Ga−I3 113.38(2), I1−Ga−N1 107.02(11), I2−Ga−N1 103.11(11), I3−Ga−N1 106.10(11).

gallium halides"[39] was concluded, the Lewis acidity order $GaCl_3$ > $GaBr_3$ > GaI_3 was found for complexes with PPh_3, dppe, and $AsMe_3$.[36−38,40,41,43]

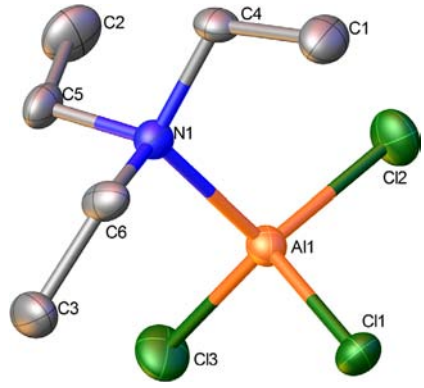

Figure 5. Molecular structure of complex **6** in the crystal. Selected interatomic distances (Å): Al1−N1 2.0181(16), Al1−Cl1 2.1684(7), Al1−Cl2 2.1837(7), Al1−Cl3 2.1714(8). Selected bond angles (deg): Cl1−Al1−Cl2 109.22(3), Cl1−Al1−Cl3 111.28(3), Cl2−Al1−Cl3 111.33(3), Cl1−Al1−N1 107.62(5), Cl2−Al1−N1 109.57(5), Cl3−Al1−N1 107.73(5).

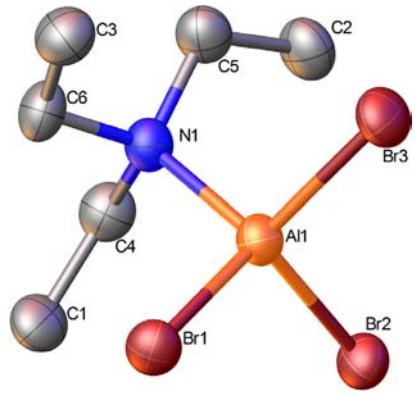

Figure 6. Molecular structure of complex **7** in the crystal (copper experiment). Selected interatomic distances (Å): Al1−N1 1.994(4), Al1−Br1 2.2875(12), Al1−Br2 2.2836(12), Al1−Br3 2.2832(14). Selected bond angles (deg): Br1−Al1−Br2 109.32(5), Br1−Al1−Br3 110.18(6), Br2−Al1−Br3110.28(5), Br1−Al1−N1 108.17(13), Br2−Al1−N1 109.68(13), Br3−Al1−N1 109.18(12).

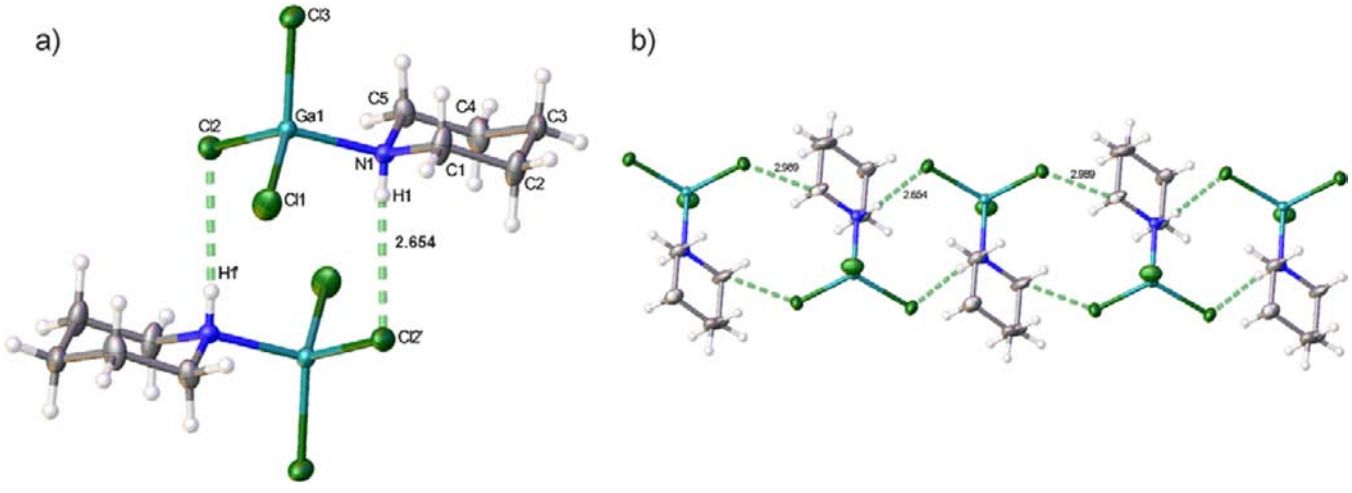

Figure 4. (a) Molecular structure of complex **5** in the crystal. (b) Packing of molecules showing the hydrogen-bonding network. Projection of the structure along the *a* axis. Selected interatomic distances (Å): Ga1−N1 1.9754(13), Ga1−Cl1 2.1539(5), Ga1−Cl2 2.1731(4), Ga1−Cl3 2.1509(4). Selected bond angles (deg): Cl1−Ga−Cl2 110.27(2), Cl1−Ga−Cl3 114.17(2), Cl2−Ga−Cl3 112.59(2), Cl1−Ga−N1 106.45(4), Cl2−Ga−N1 106.97(4), Cl3−Ga−N1 105.85(4).

dx.doi.org/10.1021/ic301507c | *Inorg. Chem.* 2012, 51, 11602−11611

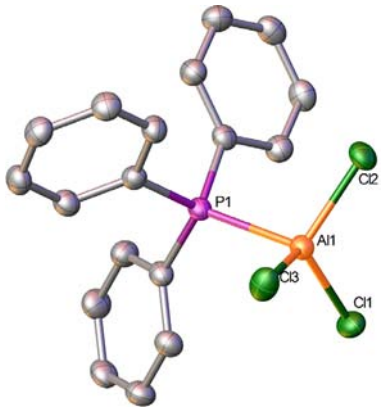

Figure 7. Molecular structure of complex **8** in the crystal. Selected interatomic distances (Å): Al1−P1 2.4296(15), Al1−Cl1 2.1224(13), Al1−Cl2 2.1140(13), Al1−Cl3 2.1079(13). Selected bond angles (deg): Cl1−Al1−Cl2 111.56(3), Cl1−Al1−Cl3 114.03(3), Cl2−Al1−Cl3 114.80(3), Cl1−Al1−P1 106.99(3), Cl2−Al1−P1 102.92(3), Cl3−Al1−P1 105.39(3).

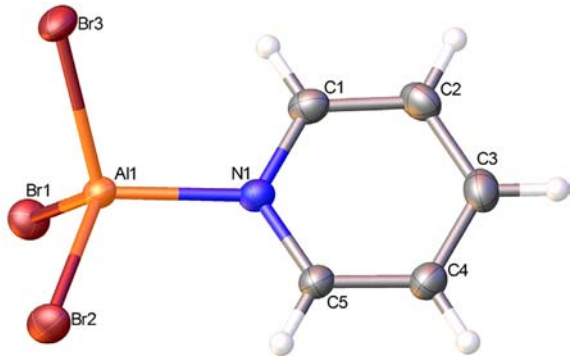

Figure 8. Molecular structure of complex **9** in the crystal. Selected interatomic distances (Å): Al1−N1 1.935(3), Al1−Br1 2.2772(10), Al1−Br2 2.2677(10), Al1−Br3 2.2796(10). Selected bond angles (deg): Br1−Al1−Br2 111.95(4), Br1−Al1−Br3 110.38(4), Br2−Al1−Br3 112.62(4), Br1−Al1−N1 107.51(9), Br2−Al1−N1 108.40(9), B3−Al1−N1 105.64(9).

The discrepancy between $P(SiMe_3)_3$ and other donors requires special attention. Experimental structural data for $AlCl_3$ and $AlBr_3$ complexes with $P(SiMe_3)_3$[31] point out that Al−P distances are essentially equal within experimental errors. The theoretically predicted M−P bond distances and dissociation energies of $AlX_3{\cdot}P(SiMe_3)_3$ and $GaX_3{\cdot}P(SiMe_3)_3$ complexes suggest that the Lewis acidity decreases in the order MCl_3 > MBr_3 > MI_3 for both aluminum and gallium halides (Table 4). Close inspection of the experimental results for $GaX_3{\cdot}P(SiMe_3)_3$ complexes reveals the presence of solvent molecules in the solid-state structures: $GaCl_3{\cdot}P(SiMe_3)_3$ cocrystallizes with C_6H_5Cl and $GaBr_3{\cdot}P(SiMe_3)_3$ with toluene. For the $GaI_3{\cdot}P(SiMe_3)_3$ complex, anomalously long P−Si [2.39(1) Å] and Si−C [2.07(5) Å] bonds are reported,[39] which casts some doubt into the validity of experimental bond distances for this compound. It may be argued that the reversed order of Lewis acidity, observed in work in ref 39, is an artifact of the presence of solvent molecules in crystal structures of $GaCl_3{\cdot}P(SiMe_3)_3$ and $GaBr_3{\cdot}P(SiMe_3)_3$, combined with some experimental inaccuracies for $GaI_3{\cdot}P(SiMe_3)_3$. Thus, on the basis of experimental structural data and theoretical results, we conclude that the order of the Lewis acidity of gallium halides is $GaCl_3$ > $GaBr_3$ > GaI_3 for all donors investigated.

Lewis Acidity Trends for Aluminum Trihalides. Molecular structures of **6** and **7** are given in Figures 5 and 6, respectively. Another polymorph of $AlBr_3{\cdot}NEt_3$ was reported before;[30] crystals of this compound were obtained from a *n*-heptane solution. Obtained in the present work at 123(1) K, the value of the Al−N distance for **7** of 1.994(4) Å is by 0.021 Å longer than the previously reported value of 1.973(8) Å at 293(2) K.[30] However, redetermined at 253(1) K, the Al−N distance is 1.977(4) Å, which agrees well with the formally reported data.[30]

The X-ray structure of the triphenylposphine adduct of $AlCl_3$ (**8**) reveals a staggered arrangement of the chlorine atoms and phenyl groups. The Al−P bond length [2.4296(15) Å] is elongated compared to the compound carrying $SiMe_3$ groups at the phosphorus atom [2.392(4) Å].[31] With 1.935(3) Å in **9**, the Al−N distance is close to the corresponding bond length of 1.930(2) Å in its isostructural chlorine derivative $AlCl_3{\cdot}Py$.[27]

Analysis of the available structural data (Table 2) reveals that AlI_3 complexes have longer Al−N DA bonds in the solid state compared to $AlCl_3$ and $AlBr_3$. Thus, AlI_3 is the weakest Lewis acid among the aluminum trihalides. This agrees well with the results of theoretical computations. However, the situation with $AlCl_3$ and $AlBr_3$ is controversial. The Al−N distance in **7** is considerably (by 0.024 Å) shorter than that in **6**, indicating that $AlCl_3$ is a weaker Lewis acid than $AlBr_3$. DA bond distances for $AlBr_3$ complexes with mdta, NEt_3, and 9-fluorenone are by 0.011, 0.024, and 0.031 Å *shorter* than those of $AlCl_3$; for other donors, they are equal within experimental errors (Table 2), with the THF complex being the only exception, for which the DA bond toward $AlBr_3$ is by 0.025 Å *longer* than that for $AlCl_3$. Thus, taking the DA bond distance as a criterion, the order of the acceptor ability will be $AlBr_3$ > $AlCl_3$.

The results of theoretical studies (Table 4) allow us to trace the influence of the acceptor and donor on the DA bond distances in gaseous complexes. For complexes of the same structural type, the computed M−N distance increases in the order $AlCl_3$ < $AlBr_3$, which agrees with a lowering of the acceptor strength of the group 13 halides. Computations predict a DA bond lengthening on going from $AlCl_3$ to $AlBr_3$, in line with a decrease of the dissociation enthalpies. Both factors suggest stronger Lewis acidity of gaseous $AlCl_3$ compared to $AlBr_3$. Only in the case of 9-fluorenone the the Al−N bond distance in $AlBr_3$·fluorenone by 0.001 Å shorter than that in $AlCl_3$·fluorenone, but the dissociation enthalpies follow the order $AlCl_3$ > $AlBr_3$. Theoretically predicted trends in bond distances are very similar for PPh_3 and $P(SiMe_3)_3$ donor ligands for both AlX_3 and GaX_3.

A comparison of the experimental (solid state; Table 2) and computed (gas phase; Table 4) bond distances allows us to analyze trends upon condensation of the complexes. Theoretically predicted M−N and M−X bond distances for the gas-phase compounds are longer than the experimentally determined distances for the solid-state adducts. This is usual because (i) it is known that the bond distances are overestimated at the B3LYP level of theory[16] (as may be seen upon comparison with gas-phase electron diffraction data for $MX_3{\cdot}NH_3$ complexes in Table 1) and (ii) for strong complexes, DA bond distances in the solid state are by 4.3% shorter compared to the gas phase,[21] which can be explained by the dipolar enhancement mechanism of Leopold et al.[58] Note that weaker complexes undergo much larger structural changes upon condensation from the gas phase to the solid state.

The differences between theoretical predictions for the gas phase and experimentally observed DA bond distances in the

dx.doi.org/10.1021/ic301507c | *Inorg. Chem.* 2012, 51, 11602−11611

Table 4. Theoretically Predicted DA Bond Distances (R_{M-D}, Å) and Standard Dissociation Enthalpies ($\Delta_{diss}H°_{298}$, kJ mol^{-1}) for Group 13 Metal Halides at the B3LYP/TZVP (def2-TZVP on I) Level of Theory

		R_{M-D}			$\Delta_{diss}H°_{298}$		
DA bond	complex	X = Cl	X = Br	X = I	X = Cl	X = Br	X = I
Al−N	AlX_3·Py	2.009	2.016	2.030	147.6	137.1	
	AlX_3·NH_3	2.022	2.024	2.036	143.7	135.9	122.9
	AlX_3·NEt_3	2.064	2.080	2.104	121.3	105.5	81.4
	AlX_3·tmpH	2.103	2.125	2.156	103.4	84.7	58.0
	ax-AlX_3·mdta	2.101	2.120	2.150	100.6	86.5	65.3
	eq-AlX_3·mdta	2.070	2.085	2.112	109.7	97.3	79.0
	ax-AlX_3·pip	2.027	2.038		146.1	134.2	
	eq-AlX_3·pip	2.013	2.024		157.3	147.4	
Al−P	AlX_3·$P(SiMe_3)_3$	2.459	2.470	2.493	120.9	109.1	88.1
	AlX_3·PPh_3	2.488	2.498	2.520	103.8	94.8	78.9
Al−O	AlX_3·THF	1.913	1.920	1.932		118.7	
	AlX_3·9-fluorenone (C_s)	1.882	1.881	1.884	117.8	108.0	92.7
Ga−O	GaX_3·9-fluorenone (C_s)	2.022	2.036	2.067	78.4	65.0	47.6
	GaX_3·THF	2.033	2.050	2.082	93.3	80.5	62.9
Ga−N	GaX_3·Py	2.071	2.086	2.112	122.0	108.3	
	GaX_3·NH_3	2.097	2.105	2.127	118.1	106.5	91.1
	GaX_3·tmpH	2.160	2.194	2.253	87.4	65.4	36.2
	ax-GaX_3·mdta	2.171	2.199	2.250	83.0	66.0	43.4
	eq-GaX_3·mdta	2.142	2.168	2.212	90.4	75.8	55.9
	ax-GaX_3·pip	2.092	2.110		123.7	108.7	
	eq-GaX_3·pip	2.077	2.093		133.7	120.7	
Ga−P	GaX_3·$P(SiMe_3)_3$	2.446	2.465	2.501	119.5	102.7	75.4
	GaX_3·PPh_3	2.476	2.492	2.523	99.8	86.6	67.2
Ga−As	GaX_3·$AsMe_3$	2.536	2.543	2.559	91.7	82.9	69.6

Table 5. DA Bond Shortening between the Gas Phase (Computed) and Experimental Solid-State Distances $r(X_3M-D)$[a] for Group 13 Metal Halides

DA bond	complex	X = Cl	X = Br	X = I
Al−N	AlX_3·NH_3	0.101	0.106	0.079
	AlX_3·tmpH	0.089	0.116	0.118
	AlX_3·Py	0.079	0.081	
	eq-AlX_3·mdta	0.077	0.103	
	AlX_3·NEt_3	0.046	0.086	
Al−P	AlX_3·$P(SiMe_3)_3$	0.067	0.079	
	AlX_3·PPh_3	0.059		
Al−O	AlX_3·THF	0.115	0.097	
	AlX_3·9-fluorenone	0.095	0.125	
	mean Al−D	0.081	0.099	0.099
Ga−O	GaX_3·9-fluorinone	0.107	0.100	
Ga−N	GaX_3·Py	0.105	0.107	0.112
	eq-GaX_3·pip	0.102		
Ga−P	GaX_3·PPh_3	0.104	0.106	
	GaX_3·$P(SiMe_3)_3$	0.066	0.103	0.154
Ga−As	GaX_3·$AsMe_3$	0.103	0.105	0.121
	mean Ga−D	0.104	0.104	0.116

[a] $\Delta r = r$(M−D; gas phase, B3LYP/TZVP) − r(M−D; solid, X-ray).

solid state are given in Table 5. Note that for gallium compounds the mean bond shortening is not dependent on the donor and is about 0.104 Å for both gallium trichloride and gallium tribromide. For aluminum complexes, Al−N bond shortening is more pronounced in bromide systems. The Al−N distances are almost equal in the gas phase (with $AlCl_3$ having slightly shorter DA bonds), but condensation reverses the order, and $AlBr_3$ forms shorter bonds. Thus, condensation is responsible for the change of the bond trend!

Why do complexes of aluminum tribromide with nitrogen-, phosphorus-, and oxygen-containing donors possess shorter or similar DA bonds in the solid state compared to those of aluminum trichloride? There are several factors that can be taken into account. One of them is the difference in reorganization energies. Upon complexation, planar MX_3 adopts a tetrahedral environment, which requires the pyramidalization energy of the acceptor molecule. On the basis of Gillespie and Popelier's ligand close-packing model,[57] the pyramidalization energy is expected to be less important with an increase of the M−X distance. Thus, longer M−X bonds provide less strain upon pyramidalization and favor shorter DA bond distances. The large pyramidalization energy of boron trihalides is one of the factors that is responsible for the increase of the Lewis acidity in the order $BF_3 < BCl_3 < BBr_3 < BI_3$.[15c] Computed pyramidalization energies (energies required to distort planar MX_3 to a perfect tetrahedral angle) for aluminum and gallium halides are given in Table 6 for both relaxed and rigid M−X bond distances. Note that the pyramidalization energies for $AlCl_3$ and $AlBr_3$ differ by less than 5 kJ mol^{-1}. This difference is expected to be even lower in the case of much smaller structural transformations, found for the solid-state adducts. Thus, the pyramidalization energy of MX_3 cannot explain the observed bond shortening in the solid $AlBr_3$·D complexes.

Temperature Factor for the DA Bond Distances. In order to understand the effect of the temperature on the DA bond distance, temperature-dependent measurements were performed for **7** at 100(1), 123(1), 153(1), 203(1), and 253(1) K. The results are summarized in Table 7. Changes in the structural parameters for **7** are marginal; the volume of the cell increases by 2.5%, with major contribution from the *a* axis. However, Al−N distances in the 100−203 K range are within experimental errors, and only at 253 K is a slight shortening of the Al−N

dx.doi.org/10.1021/ic301507c | Inorg. Chem. 2012, 51, 11602−11611

Table 6. Pyramidalization Energies of MX_3 (kJ mol^{-1}) at the B3LYP/TZVP (def2-TZVP on I) Level of Theory[a]

compound	X = F	X = Cl	X = Br	X = I
AlX_3(tetrahedral)	90.0 (90.5)	79.0 (79.9)	74.5 (75.7)	67.4 (68.5)
GaX_3(tetrahedral)	77.5 (78.0)	73.6 (74.7)	70.2 (71.6)	64.3 (66.2)

[a]Values in parentheses are for nonrelaxed pyramidalization energies (M−X bond distances are fixed at optimized values for planar MX_3).

Table 7. Temperature Dependence of Structural Parameters for 7 (Mo Kα Radiation If Not Indicated Otherwise)

T, K	a, Å	b, Å	c, Å	V, Å^3	R_{Al-N}, Å	R_{Al-Br1}, Å	R_{Al-Br2}, Å	R_{Al-Br3}, Å	Br···H, Å	Br···H, Å
100	13.4428(8)	7.3325(3)	12.0808(6)	1190.80(10)	1.989(4)	2.2851(14)	2.2858(14)	2.2841(15)	2.957, 2.974	3.011, 3.021
123	13.4728(7)	7.3315(3)	12.0931(5)	1194.51(9)	1.984(4)	2.2783(14)	2.2847(13)	2.2833(15)	2.967, 2.972	3.017, 3.020
123(Cu)	13.4888(2)	7.3348(1)	12.1051(2)	1197.65(3)	1.994(4)	2.2875(12)	2.2836(12)	2.2832(14)	2.963, 2.975	3.031, 3.039
153	13.4804(8)	7.3180(3)	12.0869(6)	1192.37(10)	1.987(5)	2.2721(18)	2.2789(17)	2.2816(19)	2.972, 2.977	3.028, 3.032
203	13.5724(7)	7.3292(3)	12.1407(5)	1207.69(9)	1.986(5)	2.2714(18)	2.2783(17)	2.2822(18)	2.965, 2.966	3.039
253	13.6452(9)	7.3395(3)	12.1837(6)	1220.19(11)	1.977(4)	2.2702(16)	2.2785(15)	2.2800(17)	2.987	3.001

Table 8. PAs (kJ mol^{-1}) of Donor Molecules, Major Bond Distances (Å), Standard Dissociation Enthalpies $\Delta_{diss}H°_{298}$ (kJ mol^{-1}), Bond Energies E_{DA} (kJ mol^{-1}), Atomic Charges on Nitrogen Atoms q_N, and Charge-Transfer Values q_{CT} for Selected $GaCl_3$·D Complexes (*eq* and *ax* Are Equatorial and Axial Isomers, Respectively)

		r(Ga−N)		r(Ga−Cl)		$\Delta_{diss}H°_{298}$				
complex	PA[44]	exp	theor	exp	theor	exp	theor	E_{DA}	q_N	q_{CT}
$GaCl_3$·Py (**1**)	930	1.966(2)	2.071	2.1502(2)	2.185	139 ± 2	122	167	−0.134	0.263
				2.1587(1)	2.188					
				2.1599(1)	2.188					
eq-$GaCl_3$·pip (**5**)	954	1.9754(13)	2.077	2.1539(5)	2.188		134	186	−0.303	0.271
				2.1731(4)	2.191					
				2.1509(4)	2.191					
ax-$GaCl_3$·pip	954		2.092		2.185, 2.194, 2.194		124	183	−0.328	0.269
$GaCl_3$·NH^iPr_2	972	2.000(3)[60]	2.129	2.146, 2.154, 2.178[60]	2.194, 2.194, 2.201		99	183	−0.346	0.241

distance (by 0.01 Å) observed. There is a tendency of a slight shortening of the Al−Br distance upon heating as well. This brings the Al−N distance of 1.977(4) Å at 253(1) K close to 1.973(8) Å reported by Schnökel et al. at 293(2) K.[30] In a previous temperature-dependent study of the $GaCl_3$·PMe_3 complex (eclipsed conformation in the solid state), changes in both the Ga−P and Ga−Cl distances from 223 to 297 K were also within experimental errors.[9] We conclude that the temperature affects the bond distances only to a small degree.

Influence of the Hydrogen Bonds on the DA Bond Distances. Another well-known factor that affects the DA bond distances in the solid state is the presence of hydrogen bonds. Structures of complexes of group 13 metal trihalides with ammonia and primary and secondary amines exhibit short N−H···X intermolecular contacts.[26,59,60] The formation of 3D networks connected via N−H···X hydrogen bonds is well-known for ammonia complexes.[26,59]

In order to study the influence of hydrogen bonds on the length of the DA bond in detail, the structure of **5** was determined in the present work. In contrast to the ionic structure $[GaCl_2pip_2]^+[GaCl_4]^-$, postulated in an earlier work on the basis of conductivity measurements,[55a] the present X-ray structural study revealed that **5** possesses a molecular structure (equatorial isomer) in the solid state (Figure 4a). An interesting feature of the $GaCl_3$·pip complex is the hydrogen-bonding network (Figure 4b). Two molecules form a head-to-tail dimer $\{GaCl_3$·$pip\}_2$ with two N−H···Cl hydrogen bonds of 2.652 Å. Moreover, these $\{GaCl_3$·$pip\}_2$ dimers are lined in the infinite chain by additional C−H···Cl intermolecular contacts of 2.927 Å. The Ga−N bond distance in **5** is 1.975 Å, which is by 0.009 Å longer compared to 1.966 Å in **1**. According to the bond energy−bond length relationship, such Ga−N distances indicate the stronger donor ability of Py. However, PA of pip is by 24 kJ mol^{-1} larger than that of Py (Table 2). Thus, we conclude that the hydrogen-bonding network leads to an elongation of the DA bond distance in the solid state.

Analogous to **5**, the $GaCl_3$·NH^iPr_2 complex also features head-to-tail dimerization with N−H···Cl hydrogen bonds of 2.570 Å.[60] The Ga−N bond distance of 2.000(3) Å in $GaCl_3$·NH^iPr_2 is even longer than that in **5**. In both **5** and $GaCl_3$·NH^iPr_2, the Ga−Cl bond distance involving the Cl atom participating in the H···Cl interaction is increased by about 0.02−0.03 Å compared to the other Ga−Cl distances (**5**, 2.173 Å vs 2.151 and 2.154 Å; $GaCl_3$·NH^iPr_2, 2.178 Å vs 2.146 and 2.154 Å). Two C−H···Cl contacts (2.814 and 2.844 Å) are present in the $GaCl_3$·Py adduct, which compare well with the one C−H···Cl contact of 2.927 Å in **5**. Such contacts do not have a noticeable effect on the Ga−Cl bond distances in **1**.

Theoretically predicted structural and energetic parameters are also summarized in Table 8. Optimized geometries of axial and equatorial isomers of the $GaCl_3$·pip complex are given in Figure 9. In agreement with the experimental findings of the equatorial isomer for the solid adduct, theoretical computations predict that the equatorial isomer (Figure 9b) is by 10 kJ mol^{-1} more stable than the axial one (Figure 9a). Note that the Ga−N bond distances in these isomers are markedly different (the Ga−N distance in the more stable equatorial isomer is by 0.015 Å shorter).

We must point out that theoretically predicted bond distances in the gas phase also increase from **1** to **5**, in agreement with the experimental data in the solid state. However, dissociation enthalpies and bond energies are increasing in accordance

dx.doi.org/10.1021/ic301507c | Inorg. Chem. 2012, 51, 11602−11611

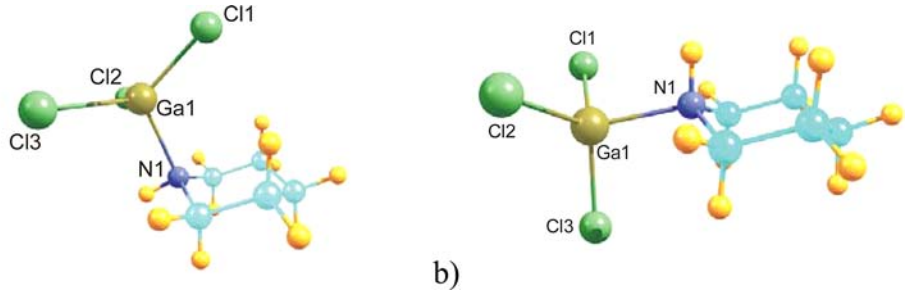

Figure 9. Structure of MX_3·pip complexes, theoretically considered in the present work as the example of $GaCl_3$·pip: (a) axial isomer; (b) equatorial isomer.

with the PA values for the donor molecules. Shorter but weaker DA bonds are known.[61] Larger stability of the pip complex compared to Py may result from larger ionic contribution, as indicated by the increased atomic charge at the nitrogen atom of piperidine (Table 8). In the gas phase, $GaCl_3$·NH^iPr_2 adopts a staggered conformation and has significantly larger reorganization energies, leading to a smaller dissociation enthalpy of the complex.

Model To Explain Observed Structural Trends. Several factors affecting the structural features of complex compounds in the solid state were discussed in Linert and Gutmann's review.[62] Analysis of the experimental structural data reveals that hydrogen-bonding networks increase the DA bond distances (vide supra). We propose that H···Cl contacts in the H···Cl–Al–D fragments lead to a partial charge transfer from Cl to H that lengthens the Cl_3Al–D bond. Analogous H···Br interactions are weaker, and the Br_3Al–D bond elongation is smaller. Because the DA bond distances in the gas phase are very close for Cl_3Al–D and Br_3Al–D, intermolecular interactions play a decisive role, which leads to shorter Br_3Al–D bond distances compared to Cl_3Al–D in the solid-state complexes. It would be interesting to see whether a similar effect is present for other donors (for example, sulfur- and selenium-containing donors) as well as for ionic complexes. This would require additional studies. We must point out that Lewis acidity trends, derived from structural data in the condensed phase, should be used with caution.

CONCLUSIONS

On the basis of experimental bond distances in the solid state, the following trend of the Lewis acidity of gallium trihalides toward pyridine was established: $GaCl_3$ > $GaBr_3$ > GaI_3. This trend agrees well with the theoretical predictions for the corresponding gas-phase complexes. The acceptor ability of Lewis acids according to computed dissociation enthalpies decreases in the order $AlCl_3$ > $AlBr_3$ > $GaCl_3$ > $GaBr_3$. Analysis of the experimental and theoretical results points out that the solid state masks the Lewis acidity trend of aluminum halides. The difference in the Al–D bond distances between $AlCl_3$·D and $AlBr_3$·D complexes in the gas phase is small, while in the condensed phase, shorter Al–D distances for $AlBr_3$·D complexes are observed with 9-fluorenone, mdta, and NEt_3 donors. This trend can be explained on the basis of differences in intermolecular H···Cl and H···Br interactions. Thus, the DA bond distance in the solid-state complexes cannot always be used as a criterion of Lewis acidity.

ASSOCIATED CONTENT

Supporting Information

X-ray crystallographic data in CIF format, table with the total energies of the theoretically studied compounds, and figure depicting the disordered molecular structure of complex **4** in the crystal. This material is available free of charge via the Internet at http://pubs.acs.org.

AUTHOR INFORMATION

Corresponding Author

*E-mail: alextim@AT11692.spb.edu (A.Y.T.), manfred.scheer@chemie.uni-regensburg.de (M.S.).

Notes

The authors declare no competing financial interest.

ACKNOWLEDGMENTS

This work was supported by St. Petersburg State University Research Grant 12-37-139-2011. A.Y.T. is grateful to the Alexander von Humboldt Foundation for a reinvitation fellowship.

REFERENCES

(1) (a) Lewis, G. N. *Valence and the structure of atoms and molecules*, 1st ed.; Chemical Catalog Co.: New York, 1923. (b) Lewis, G. N. *J. Franklin Inst.* **1938**, *226*, 293.
(2) Szulejko, J. E.; McMahon, T. B. *J. Am. Chem. Soc.* **1993**, *115*, 7839.
(3) (a) Gutmann, V.; Wychera, E. *Inorg. Nucl. Chem. Lett.* **1966**, *2*, 257. (b) Gutmann, V. *Coordination Chemistry in Non-Aqueous Solutions*; Springer Vertag: Wienheim, Germany, 1969. (c) Gutmann, V. *Coord. Chem. Rev.* **1976**, *18*, 225.
(4) Mayer, U.; Gutmann, V.; Gerger, W. *Monatsh. Chem.* **1975**, *106*, 1235.
(5) (a) Satchell, D. P. N.; Satchell, R. S. *Chem. Rev.* **1969**, *69*, 251. (b) Bukka, K.; Satchell, R. S. *J. Chem. Soc., Perkin Trans. 2* **1976**, 1058. (c) Mohammad, A.; Satchell, D. P. N. *J. Chem. Soc. B* **1968**, 331. (d) Mohammad, A.; Satchell, D. P. N. *J. Chem. Soc. B* **1967**, 726.
(6) Hargittai, M.; Hargittai, I. *The Molecular Geometries of Coordination Compounds in the Vapour Phase*; Elsevier: Amsterdam, The Netherlands, 1977.
(7) Henrici-Olive, G.; Olive, S. *J. Organomet. Chem.* **1969**, *17*, 83.
(8) Hilt, G.; Pünner, F.; Möbus, J.; Naseri, V.; Bohn, M. A. *Eur. J. Org. Chem.* **2011**, 5962.
(9) Carter, J. C.; Jugie, G.; Enjalbert, R.; Galy, J. *Inorg. Chem.* **1978**, *5*, 1248.
(10) (a) Lappert, M. F. *J. Chem. Soc.* **1962**, 542. (b) Shriver, D. F.; Swanson, B. *Inorg. Chem.* **1971**, *10*, 1354. (c) Ford, T. A. *J. Mol. Struct.* **2007**, *834–836*, 30.
(11) Guryanova, E. N.; Goldshtein, I. P.; Romm., I. P. *Donor–Acceptor Bond*; John Wiley and Sons: New York, 1975; p 366.

(12) Doolan, P. C.; Gore, P. H.; Waters, D. N. *J. Chem. Soc., Perkin Trans. 2* **1974**, 241.
(13) Branch, C. S.; Bott, S. G.; Barron, A. R. *J. Organomet. Chem.* **2003**, *666*, 23.
(14) Ogawa, A.; Fujimoto, H. *Inorg. Chem.* **2002**, *41*, 4888.
(15) (a) Rowsell, B. D.; Gillespie, R. J.; Heard, G. L. *Inorg. Chem.* **1999**, *38*, 4659. (b) Hirao, H.; Omoto, K.; Fujimoto, H. *J. Phys. Chem. A* **1999**, *103*, 5807. (c) Bessac, F.; Frenking, G. *Inorg. Chem.* **2003**, *42*, 7990. (d) Franca, C. A.; Diez, R. P. *J. Argent. Chem. Soc.* **2009**, *97*, 119.
(16) Timoshkin, A. Y.; Suvorov, A. V.; Bettinger, H. F.; Schaefer, H. F. *J. Am. Chem. Soc.* **1999**, *121*, 5687.
(17) Hargittai, M.; Hargittai, I.; Spiridonov, V. P.; Ivanov, A. A. *J. Mol. Struct.* **1977**, *39*, 225.
(18) Hargittai, M.; Hargittai, I.; Spiridonov, V. P. *J. Mol. Struct.* **1976**, *30*, 31.
(19) Hargittai, M.; Hargittai, I.; Spiridonov, V. P.; Pelissier, M.; Labarre, J. F. *J. Mol. Struct.* **1975**, *24*, 27.
(20) Shubaev, V. L. Cand. Sci. Thesis, Leningrad State University, Leningrad, Russia, 1971.
(21) Davydova, E. I.; Sevastianova, T. N.; Suvorov, A. V.; Timoshkin, A. Y. *Coord. Chem. Rev.* **2010**, *254*, 2031.
(22) Trusov, V. I.; Suvorov, A. V. *Zh. Neorg. Khim.* **1974**, *19*, 3253.
(23) Trusov, V. I.; Suvorov, A. V.; Abakumova, R. N. *Zh. Neorg. Khim.* **1975**, *20*, 501.
(24) Trusov, V. I.; Suvorov, A. V.; Tarasova, A. S. *Zh. Neorg. Khim.* **1976**, *21*, 3102.
(25) Romm, I. P.; Noskov, Y. G.; Malkov, A. A. *Russ. Chem. Bull.* **2007**, *56*, 1935.
(26) Jacobs, H.; Schroder, F. O. *Z. Anorg. Allg. Chem.* **2002**, *628*, 327.
(27) Dimitrov, A.; Heidemann, D.; Kemnitz, E. *Inorg. Chem.* **2006**, *45*, 10807.
(28) Krossing, I.; Nöth, H.; Schwenk-Kircher, H.; Seifert, T.; Tacke, C. *Eur. J. Inorg. Chem.* **1998**, 1925.
(29) Gálvez-Ruiz, J. C.; Guadarrama-Pérez, C.; Nöth, H.; Flores-Parra, A. *Eur. J. Inorg. Chem.* **2004**, 601.
(30) Vollet, J.; Burgert, R.; Schnöckel, H. *Angew. Chem., Int. Ed.* **2005**, *44*, 6956.
(31) Wells, R. L.; McPhail, A. T.; Laske, J. A.; White, P. S. *Polyhedron* **1994**, *13*, 2737.
(32) Burford, N.; Royan, B. W.; Spence, R. E. v. H.; Cameron, T. S.; Linden, A.; Rogers, R. D. *J. Chem. Soc., Dalton Trans.* **1990**, 1521.
(33) Engelhardt, L. M.; Junk, P. C.; Raston, C. L.; Skelton, B. W.; White, A. H. *J. Chem. Soc., Dalton Trans.* **1996**, 3297.
(34) Scholz, S.; Lerner, H.-W.; Bolte, M. *Acta Crystallogr., Sect. E* **2003**, *59*, m289.
(35) Boucher, D. L.; Brown, M. A.; McGarvey, B. R.; Tuck, D. G. *J. Chem. Soc., Dalton Trans.* **1999**, 3445.
(36) Cheng, F.; Codgbrook, H. L.; Hector, A. L.; Levason, W.; Reid, G.; Webster, M.; Zhang, W. *Polyhedron* **2007**, *26*, 4147.
(37) Baker, L.-J.; Kloo, L. A.; Rickard, C. E. F.; Taylor, M. J. *J. Organomet. Chem.* **1997**, *545*−*546*, 249.
(38) Brown, M. A.; Castro, J. A.; Tuck, D. G. *Can. J. Chem.* **1997**, *75*, 333.
(39) Janik, J. F.; Baldwin, R. A.; Wells, R. L.; Pennington, W. T.; Schimek, G. L.; Rheingold, A. L.; Liable-Sands, L. M. *Organometallics* **1996**, *15*, 5385.
(40) Cheng, F.; Hector, A. L.; Levason, W.; Reid, G.; Webster, M.; Zhang, W. *Acta Crystallogr., Sect. E* **2007**, *63*, m1761.
(41) Sigl, M.; Schier, A.; Schmidbaur, H. *Z. Naturforsch. B* **1998**, *53*, 1301.
(42) (a) Bantu, B.; Pawar, G. M.; Wurst, K.; Decker, U.; Schmidt, A. M.; Buchmeiser, M. R. *Eur. J. Inorg. Chem.* **2009**, 1970. (b) Ghadwal, R. S.; Roesky, H. W.; Hebst-Irmer, R.; Jones, P. G. *Z. Anorg. Allg. Chem.* **2009**, *635*, 431. (c) Marion, N.; Escudero-Adan, E. C.; Benet-Buchlolz, J.; Stevens, E. D.; Fensterbank, L.; Malacria, M.; Nolan, S. P. *Organometallics* **2007**, *26*, 3256. (d) Ball, E.; Cole, L. C.; McKay, A. I. *Dalton Trans.* **2012**, *41*, 946.
(43) Cheng, F.; Hector, A. L.; Levason, W.; Reid, G.; Webster, M.; Zhang, W. *Inorg. Chem.* **2007**, *46*, 7215.
(44) Hunter, E. P.; Lias, S. G. *J. Phys. Chem. Ref. Data* **1998**, *27*, 413.
(45) Timoshkin, A. Y.; Suvorov, A. V.; Schaefer, H. F. *Zh. Obsh. Khim.* **1999**, *69*, 1250.
(46) *CrysAlisPro Software system*, different versions; Agilent Technologies UK Ltd.: Oxford, U.K., 2006−2012.
(47) Clark, R. C.; Reid, J. S. *Acta Crystallogr.* **1995**, *A51*, 887−897.
(48) Altomare, A.; Burla, M. C.; Camalli, M.; Cascarano, G. L.; Giacovazzo, C.; Guagliardi, A.; Moliterni, A. G. G.; Polidori, G.; Spagna, R. *J. Appl. Crystallogr.* **1999**, *32*, 115−119.
(49) Palatinus, L.; Chapuis, G. *J. Appl. Crystallogr.* **2007**, *40*, 786−790.
(50) Sheldrick, G. M. *Acta Crystallogr.* **2008**, *A64*, 112−122.
(51) (a) Becke, A. D. *J. Chem. Phys.* **1993**, *98*, 5648. (b) Lee, C.; Yang, W.; Parr, R. G. *Phys. Rev. B* **1988**, *37*, 785.
(52) (a) Schafer, A.; Huber, C.; Ahlrichs, R. *J. Chem. Phys.* **1994**, *100*, 5829. (b) Krishnan, R.; Binkley, J. S.; Seeger, R.; Pople, J. A. *J. Chem. Phys.* **1980**, *72*, 650. (c) Peterson, K. A.; Figgen, D.; Goll, E.; Stoll, H.; Dolg, M. *J. Chem. Phys.* **2003**, *119*, 11113.
(53) Frisch, M. J.; Trucks, G. W.; Schlegel, H. B.; Scuseria, G. E.; Robb, M. A.; Cheeseman, J. R.; Montgomery, J. A., Jr.; Vreven, T.; Kudin, K. N.; Burant, J. C.; Millam, J. M.; Iyengar, S. S.; Tomasi, J.; Barone, V.; Mennucci, B.; Cossi, M.; Scalmani, G.; Rega, N.; Petersson, G. A.; Nakatsuji, H.; Hada, M.; Ehara, M.; Toyota, K.; Fukuda, R.; Hasegawa, J.; Ishida, M.; Nakajima, T.; Honda, Y.; Kitao, O.; Nakai, H.; Klene, M.; Li, X.; Knox, J. E.; Hratchian, H. P.; Cross, J. B.; Adamo, C.; Jaramillo, J.; Gomperts, R.; Stratmann, R. E.; Yazyev, O; Austin, A. J.; Cammi, R.; Pomelli, C.; Ochterski, J. W.; Ayala, P. Y.; Morokuma, K.; Voth, G. A.; Salvador, P.; Dannenberg, J. J.; Zakrzewski, V. G.; Dapprich, S.; Daniels, A. D.; Strain, M. C.; Farkas, O.; Malick, D. K.; Rabuck, A. D.; Raghavachari, K.; Foresman, J. B.; Ortiz, J. V.; Cui, Q.; Baboul, A. G.; Clifford, S.; Cioslowski, J.; Stefanov, B. B.; Liu, G.; Liashenko, A.; Piskorz, P.; Komaromi, I.; Martin, R. L.; Fox, D. J.; Keith, T.; Al-Laham, M. A.; Peng, C. Y.; Nanayakkara, A.; Challacombe, M.; Gill, P. M. W.; Johnson, B.; Chen, W.; Wong, M. W.; Gonzalez, C.; Pople, J. A. *GAUSSIAN 03*, revision B.05; Gaussian Inc.: Pittsburgh, PA, 2003.
(54) Sevast'yanova, T. N.; Suvorov, A. V. *Russ. J. Coord. Chem.* **1999**, *25*, 679.
(55) (a) Greenwood, N. N.; Wade, K. *J. Chem. Soc.* **1958**, 1671. (b) Greenwood, N. N.; Wade, K. *J. Chem. Soc.* **1958**, 1663.
(56) (a) Sinclair, J.; Small, R. W. H.; Worrall, I. J. *Acta Crystallogr.* **1981**, *B37*, 1290. (b) Pullman, P.; Hensen, K.; Bats, J. W. *Z. Naturforch. B* **1982**, *37b*, 1312.
(57) Gillespie, R. L.; Popelier, P. L. A. *Chemical bonding and molecular geometry*; Oxford University Press: New York, 2001; p 191.
(58) Leopold, K. R.; Canagaratna, M.; Phillips, J. A. *Acc. Chem. Res.* **1997**, *30*, 57 and references cited therein.
(59) Trinh, C.; Bodensteiner, M.; Virovets, A.; Peresypkina, E.; Scheer, M.; Matveev, S. M.; Timoshkin, A. Y. *Polyhedron* **2010**, *29*, 414.
(60) Pauls, J.; Chitsaz, S.; Neumuller, B. *Z. Anorg. Allg. Chem.* **2001**, *627*, 1723.
(61) (a) Fischer, R. A.; Schulte, M. M.; Weiss, J.; Zsolnai, L.; Jacobi, A.; Huttner, G.; Frenking, G.; Boehme, C.; Vyboishchikov, S. F. *J. Am. Chem. Soc.* **1998**, *120*, 1237. (b) Erhardt, S.; Frenking, G. *Chem.—Eur. J.* **2006**, *12*, 4620.
(62) Linert, W.; Gutmann, V. *Coord. Chem. Rev.* **1992**, *117*, 159.